A Bow-Tie Framework for Resource Adequacy and Involuntary Load Curtailment Risk

Weihui Fu, Ravi Duggirala, Pete Warnken, Adam Martinez, Richard Scheel
Electric Reliability Council of Texas, Taylor, TX, USA
Weihui.Fu@ercot.com, Ravikrishna.Duggirala@ercot.com, Pete.Warnken@ercot.com ,
Adam.Martinez@ercot.com, Richard.Scheel@ercot.com

Abstract— **This paper presents a stochastic framework based on the bow-tie methodology and root-cause analysis to assess correlated triggering risk events, combined with Monte Carlo simulation of cascading barrier failures. The example framework models root causes—including low renewable output, high thermal outages, and severe transmission constraints—and quantifies their combined impact when the Capacity Available for Operating Reserves (CAFOR) falls below 1,500 MW. Preventive and mitigative barriers, consistent with ERCOT's Energy Emergency Alert (EEA) actions, are simulated using Monte Carlo techniques with correlated reliability parameters. Results show that winter months peak near 3% involuntary load curtailment at the 95th percentile, while summer months remain at ~0.6–0.8%. The framework demonstrates a data-driven basis for evaluating resource adequacy and prioritizing reliability investments in increasingly weather-dependent grids.**

Index Terms – **Power System Reliability, Risk Assessment, Resource Adequacy, Load Curtailment, Monte Carlo Simulation**

I. Introduction

The reliable operation of power systems is increasingly challenged by rapid expansion and integration of renewables, flexible load growth such as crypto-mining and data center loads, transmission congestion constraints, and more frequent extreme weather events. These factors heighten the risk of involuntary load curtailment when generation or reserves are insufficient to meet demand. Recent ERCOT winter and summer events have highlighted the limitations of deterministic planning methods that overlook correlated risks across resources and infrastructure.

Recent national reports have raised similar concerns. The U.S. Department of Energy's grid reliability and resilience report [1] and the Energy Systems Integration Group (ESIG) guidance [2] recommend probabilistic frameworks that capture interdependent risks and stochastic resource behavior. However, few implementations explicitly align such methods with ERCOT's operational indicators such as Capacity Available for Operating Reserves (CAFOR). Traditional adequacy models [3]–[5] often rely on static reserve margins or single-contingency assumptions, underestimating compound event probabilities. Recent work on risk management for highly electrified systems emphasizes linking probabilistic risk assessment with resilience quantification and mitigation planning [6].

This paper introduces a probabilistic bow-tie framework for ERCOT that integrates root cause analysis of correlated triggering events with event-tree simulation of cascading mitigative barrier failures. The approach aligns with ERCOT's Energy Emergency Alert (EEA) procedures and quantifies percentile-based risks of load curtailment, supporting more informed reliability planning and operational decision-making. This stochastic risk framework builds upon ERCOT's Probabilistic Reserve Risk Model (PRRM), developed as an hourly risk screening tool for assessing the likelihood of ERCOT issuing Energy Emergency Alerts during the expected peak load day of a given month. The PRRM is used for ERCOT's Monthly Outlook for Resource Adequacy (MORA) reports [7]. This framework extends the PRRM by (i) bow-tie mapping of threats to preventive and mitigative actions aligned with ERCOT EEA operations, (ii) explicit copula-based modeling of correlated barrier failures, and (iii) tail-quantile (p95/p99) consequence metrics and tornado sensitivity ranking to support mitigation prioritization.

II. ERCOT EEA Protocols

ERCOT's EEA protocol [8] defines three escalating reliability actions for resource scarcity: EEA-1 (<2,500 MW reserves) activates additional generation and imports; EEA-2 (<2,000 MW or <59.91 Hz) deploys demand management; and EEA-3 (<1,500 MW or <59.8 Hz) initiates controlled load shedding. These stages correspond well to the preventive and mitigative barriers in the bow-tie methodology, with EEA thresholds embedded in the CAFOR-based framework to align the simulation with ERCOT operations.

III. Methodology

This paper adopts the bow-tie framework [9] to represent root causes, preventive and mitigative barriers, and consequences, thereby structuring the ERCOT curtailment risk pathway. Fig. 1 illustrates this framework as applied to ERCOT load curtailment risk. The model links key initiating threats, resource availability, extreme weather, market design gaps, transmission constraints, and fuel supply risk, which can jointly reduce CAFOR below 1,500 MW, triggering an EEA Level 3 event. Preventive barriers (e.g., Weatherization, Market Incentives, Transmission Upgrades) reduce the likelihood of this event, while mitigative barriers (e.g., Emergency Response Service (ERS), Reliability Unit Commitment (RUC), voltage reduction, controlled load

979-8-3315-8138-1

shedding) limit its impact. Consequences range from minor load shedding to ERCOT-wide outages and regulatory intervention.

A. CAFOR Definition and Threshold Justification

CAFOR represents the amount of dispatchable capacity ERCOT has available above current system load and committed generation [7].

$$CAFOR_t = C_t^{online+QS} - L_t - U_t + R_t^{preEEA} + R_t^{EEA} \quad (1)$$

where $C_t^{online+QS}$ is the total online and quick-start dispatchable capacity (MW), L_t is the total system demand (MW) at the same interval, U_t represents the unplanned outages and derates (MW), R_t^{PreEEA} is Pre-EEA Resources if CAFOR < 3,000 MW, and R_t^{EEA} is EEA Resources if CAFOR < 2,500 MW.

In this baseline implementation, CAFOR < 1,500 MW is represented as a calibrated indicator event defined by the occurrence of ≥1 stress triggers, rather than explicitly sampling the continuous terms in (1). Each trigger corresponds conceptually to a distinct CAFOR driver (renewable scarcity, thermal derates, load error, or deliverability constraint), and co-occurrence is handled through the correlation model to avoid double counting. Future work will compute CAFOR directly by sampling the continuous components of (1).

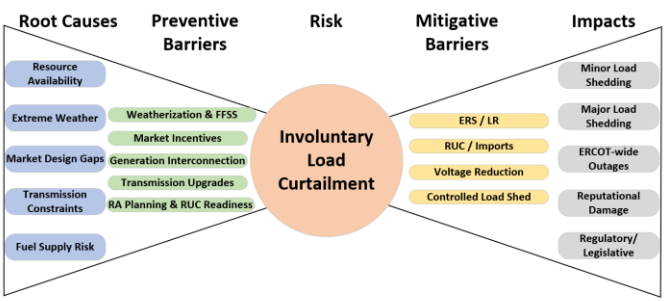

Fig. 1 Bow-Tie Framework Linking Root Causes, Preventive Barriers, Mitigative Barriers, and Impacts for ERCOT Load Curtailment Risk

B. Triggering Events (Root Cause Analysis)

This subsection defines the initiating conditions, or triggering events, that may lead to system resource inadequacy. Each trigger is represented as a correlated Bernoulli indicator generated via a Gaussian-copula latent normal vector (Cholesky-correlated), preserving specified marginal event probabilities and correlations; this does not assume the physical drivers are Gaussian. A critical risk event is declared when one or more triggering events occur within a Monte Carlo trial, indicating that the system may experience a condition of CAFOR below 1,500 MW.

The correlated random sampling process is expressed as:

$$Z = L_{trigger} \times \varepsilon, \ \varepsilon \sim N(0, I) \quad (2)$$

where Z represents the vector of correlated standard-normal random variables, and $L_{trigger}$ is the lower-triangular Cholesky factor of the trigger correlation matrix $\Sigma_{trigger}$. A critical risk event occurs when one or more trigger variables fall below their respective quantile thresholds:

$$Top\ Event = 1\left(\sum_i 1(Z_i < Z_{pi}) \geq 1\right) \quad (3)$$

Here, Z_{pi} denotes the inverse standard-normal quantile corresponding to each trigger probability p_i.

The probabilities in Table 1 are empirically derived from ERCOT operational data and seasonal studies, serving as baseline inputs for scenario calibration. While not the result of formal statistical fitting, they represent transparent, data-driven estimates consistent with observed system behavior. A one-at-a-time ±50% perturbation of individual trigger probabilities shifts the January p99 load shed by up to approximately ±0.64 percentage points for wind, solar, and thermal outage triggers, while BESS degradation and TX South interface triggers shift the January p99 by less than ±0.10 percentage points (100k trials, seed = 42). For renewable triggers, the values correspond to the lower-tail (5th-percentile) output of ERCOT's system-wide[1] wind and solar generation based on seasonal production distributions from the past decade. Thermal outage probabilities align with ERCOT's seasonal forced-outage forecasts and historical coincidence rates for extreme winter conditions. Load-forecast and transmission probabilities are calibrated from operational error statistics and congestion data, respectively. The BESS degradation case represents a stress-testing assumption intended to capture plausible but rare fleet-level reliability degradation, and it is further explored in sensitivity analysis.

This approach maintains transparent linkage between observed system performance and modeled risk inputs. The resulting baseline scenario provides a transparent, scenario-driven foundation for the subsequent Monte Carlo simulations of correlated system stress and barrier failure.

Table 1 Base triggering events and their probabilities

ID	Trigger (Basic Event)	Base Probability p_i	Threshold $Z_{pi} = \phi^{-1}(p_i)$
1	Wind output ≤ 5th percentile	0.05	−1.6449
2	Solar output ≤ 5th percentile	0.05	−1.6449
3	BESS availability reduced by 50%	0.01	−2.3263
4	Thermal outages > 20 GW	0.05	−1.6449
5	Load forecast error > 5%	0.02	−2.0537
6	TX South interface constraint[2]	0.01	−2.3263

The trigger correlation matrix includes mixed-sign dependence (e.g., wind–solar anticorrelation) with modest correlations elsewhere (typically |ρ| ≤ 0.3); Cholesky decomposition ensures realistic co-occurrence. The wind and solar power forecast error correlation was derived from wind-solar error modeling in [10], while the other values were informed by ERCOT forced outage historical data.

C. Root Cause Analysis and Impact Analysis Integration

To reflect the cascading nature of reliability risks, the framework integrates root cause analysis of triggering events with impact analysis of mitigation failures. The root cause

[1] This implementation uses system-wide ERCOT wind and solar data for risk estimation, while the PRRM (MORA model) applies separate coastal and non-coastal wind distributions. Future updates will add regional modeling for more detailed risk assessment.

[2] Other major interfaces were not explicitly modeled in this version; future work will expand the network representation.

979-8-3315-8138-1

analysis estimates the probability of CAFOR dropping below 1,500 MW due to correlated risks. If this threshold is breached, the impact analysis simulates the outcomes of mitigative barrier failures and quantifies the resulting load shed.

D. Barrier Probability and Correlation Implementation

To realistically represent the behavior of ERCOT's preventive and mitigative reliability barriers, the simulation incorporates both individual failure probabilities and cross-barrier correlations that reflect historical co-dependencies observed in system stress events. These two elements govern how the event-tree portion of the Monte Carlo framework propagates cascading risk once a critical risk event (CAFOR < 1,500 MW) is triggered.

1. Barrier Failure Probabilities

Each barrier, whether preventive (e.g., Weatherization, Market Incentives, Transmission Upgrade, Interconnection) or mitigative[3] (e.g., ERS, RUC, Load Shedding, Voltage Reduction, FFSS), is assigned a base failure probability ρ_i, representing the likelihood that the barrier fails to perform when challenged by a system stress condition. These probabilities are derived from a combination of historical performance data, expert judgment, and policy-driven assumptions, and are parameterized in the simulation such as:

$$\rho = [0.05, 0.10, 0.08, 0.12, 0.10, 0.10, 0.05, 0.02, 0.10] \tag{4}$$

where each element corresponds respectively to the barriers listed above.

To capture seasonal variability, the model modifies certain barrier probabilities monthly. The most notable seasonal adjustment is for Weatherization, whose failure probability is elevated to 0.20 in January and 0.18 in December to reflect winter exposure, while set to zero in mild months where weather stress is negligible. This adjustment aligns with ERCOT's operational observations that winterization measures are most critical during extreme cold events.

For each simulation trial, these probabilities represent the conditional likelihood of barrier failure, given that the system has already entered an emergency state (i.e., the critical risk event has occurred). If no critical risk event is triggered, all barrier failure probabilities are set to zero, effectively bypassing the event-tree stage. This conditional activation ensures that barriers are evaluated only under system stress, consistent with bow-tie logic, where preventive defenses are challenged only when upstream root causes materialize.

2. Barrier Correlation Modeling

In practice, mitigative barriers do not fail independently. Systemic stresses, such as extreme weather, regional fuel shortages, or widespread equipment derates, can cause multiple defenses to degrade within a Monte Carlo trial. To represent cross-barrier dependencies, we construct a symmetric 9×9 correlation matrix with banded coefficients ($\rho \approx 0.7$–0.85 for operationally coupled barriers, $\rho \approx 0.4$–0.6 for moderately related barriers, and $\rho < 0.3$ otherwise). We generate correlated binary failure outcomes using a Gaussian-copula approach: draw a standard-normal vector with the specified correlation (via Cholesky decomposition), then map each component to a failure indicator by comparing it to the inverse-CDF quantile implied by that barrier's failure probability. This produces realistic joint-failure behavior while preserving positive-semidefinite correlation structure. For example, strong correlations (0.7–0.85) link Weatherization, Fuel Supply, and Transmission (e.g., ρ(Weatherization, FFSS) = 0.85 in the baseline), reflecting how a prolonged cold front can simultaneously impact gas delivery, plant operability, and network capacity. Moderate correlations (0.4–0.6) connect Market Incentives, RUC, and ERS, reflecting shared exposure to dispatch and market conditions. Weaker correlations (< 0.3) apply to operationally independent barriers such as Voltage Reduction. Empirical correlation estimates between mitigative barriers remain limited. Current parameterizations are based on banded correlation ranges informed by operator judgment and qualitative event reviews. Further work will use historical emergency event logs and post-event reports to empirically derive correlated mitigation failure rates.

3. Conditional and Dynamic Adjustments

During each Monte Carlo iteration, barrier failure probabilities may be conditionally adjusted based on triggering events (e.g., simultaneous low wind and solar output increases risk for Weatherization or ERS). All reported baseline results (Figs. 2–5 and Table 2) use $\Delta p = 0$ (no trigger-conditioned increments); conditional adjustments are supported by the framework but disabled in the baseline runs.

4. Role in the Impact Analysis

Once the correlated barrier failures are generated, each failed barrier contributes a random load-shed impact drawn from a $Normal(\mu, \sigma)$ distribution with barrier-specific parameters (e.g., 3 GW ± 0.5 GW for major structural defenses, 1 GW ± 0.2 GW for responsive mitigations). The aggregate load shed in each trial is then normalized by the monthly peak demand to produce a percentage of system load curtailed.

By repeating this process across a large number of simulation trials per month, the model yields a probabilistic distribution of load-shed severity that directly reflects the interplay between barrier reliability and barrier correlation.

5. Interpretation

This dual-layer approach—combining probabilistic barrier failure with correlated dependencies—ensures that the impact analysis does not underestimate compound risks. It acknowledges that, in reality, a single weather- or market-driven stressor within a Monte Carlo trial can degrade multiple defensive layers. As a result, the load-shed distribution captures both the likelihood and the compounding severity of concurrent barrier degradations, forming the quantitative foundation for the percentile-based risk metrics illustrated in the following simulation examples.

E. Peak Load Forecasts

Example monthly peak load estimates are sourced from ERCOT operational planning data [11]. These values are used

[3] Energy Storage Resources (ESRs) enhance flexibility via state-of-charge management and can significantly reduce scarcity. Though not yet included, ESR flexibility will serve as a dynamic mitigative barrier in future versions.

979-8-3315-8138-1

to normalize load-shed impacts and assess risk relative to system demand.

F. *Sensitivity and Scenario Analysis*

To assess the robustness of the risk framework, we conduct scenario analyses by varying barrier failure probabilities and correlation strengths. This enables evaluation of mitigation effectiveness and identification of critical risk drivers.

G. *Statistical Assumptions*

For this initial implementation, normally distributed residuals were used to simplify parameter estimation and facilitate correlation modeling across multiple triggers and barriers. Sensitivity to heavy-tailed dependence was evaluated by replacing the Gaussian copula used for correlated barrier failures with a Student-t copula (df=4), which increased the January p99 load shed from 9.95% to 10.49% of peak load (100k trials, seed=42). Future work will extend the framework to mixed Normal–GEV formulations for outage magnitudes, renewable shortfalls, and extreme weather-driven deviations, consistent with ERCOT's PRRM methodology [7].

H. *Simulation Setup Summary*

The overall simulation combines correlated triggering-event sampling, conditional activation of preventive and mitigative barriers, copula-based modeling of correlated barrier failures, and Monte Carlo aggregation of load-shed impacts. Monthly simulations use 100,000 trials with a fixed random seed to ensure reproducibility, and results are reported as percentile-based risk metrics normalized to monthly peak load.

IV. Simulation Results

To demonstrate the application of the proposed probabilistic framework, a 12-month Monte Carlo simulation was conducted, comprising 100,000 trials per month. The simulation incorporated correlated risk events and mitigative barrier failures, with parameters aligned to peak-load forecasts and seasonal variations in barrier reliability.

A. *Monthly Load Shed Risk Distribution*

Fig. 2 summarizes the monthly 95th-percentile load-shed risk as a percentage of system peak demand. Results show that winter and summer months exhibit the highest risk concentrations, corresponding to periods of extreme temperature and stressed resource conditions. Overall, January and December represent the most vulnerable months, with the 95th-percentile load shed exceeding 2.5–3.5% of system demand, primarily due to elevated weatherization failure probabilities and correlated renewable shortfalls. Mid-summer months (June–August) show smaller but non-negligible risks (0.6–0.8%), reflecting transmission and thermal-outage sensitivities under high-load conditions.

Table 2 presents the monthly distribution of simulated load shed as a percentage of peak system load, based on a Monte Carlo analysis of triggering events and impacts of mitigative barriers. For each month, the table reports the peak load (GW) along with the 50th, 90th, 95th, and 99th percentile values of load shed risk. Because the stress-trigger indicator is infrequent and barriers often succeed, the p50 and p90 outcomes are zero in the baseline.

B. *Annual Cumulative Distribution*

As shown in Fig. 3, when combining all months, the annual cumulative distribution function (CDF) of total load-shed probability exhibits a long tail. The median (50th percentile) risk corresponds to negligible load loss (< 0.1%). The 95th percentile represents approximately 0.8–1.0% annualized risk. Extreme events in the 99th percentile could result in load curtailments exceeding 7–9% of system load, consistent with severe winter storm scenarios.

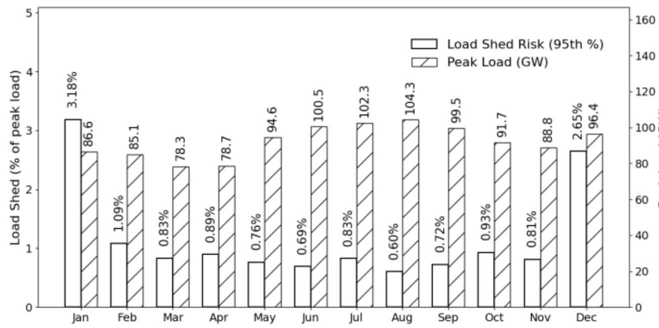

Fig. 2 Monthly Load Shed Risk vs. Peak Load Forecast (2027)

Table 2 Monthly Load Shed Percentile Summary Table

Month	Peak Load (GW)	50th%	90th%	95th%	99th%
Jan	86.64	0	0	3.18	9.95
Feb	85.07	0	0	1.09	8.92
Mar	78.3	0	0	0.83	8.51
Apr	78.67	0	0	0.89	8.61
May	94.64	0	0	0.76	7.17
Jun	100.49	0	0	0.69	6.81
Jul	102.33	0	0	0.83	6.68
Aug	104.29	0	0	0.6	6.4
Sep	99.54	0	0	0.72	6.88
Oct	91.75	0	0	0.93	7.5
Nov	88.82	0	0	0.81	7.6
Dec	96.38	0	0	2.65	8.94

C. *Correlation and Barrier Sensitivity*

Correlation analysis confirms that concurrent renewable generation shortfalls and elevated thermal outages substantially increase the probability of CAFOR falling below 1,500 MW, with Weatherization, FFSS, and ERS barriers most strongly correlated under winter stress. In January, the 95th-percentile load shed is ~3.1% of peak load and the 99th ~10% under base Weatherization failure probability (0.20); improving Weatherization reliability by 50% ($p = 0.10$) lowers the 95th to ~1.3% (Fig. 4). Reducing the correlation between Weatherization and Fuel Supply (FFSS) from $\rho = 0.85$ to $\rho = 0.50$ changes the January p99 load shed from 9.95% to 9.84% of peak load (100k trials, seed = 42), indicating limited sensitivity of p99 to this single coupling under the baseline parameterization. Improvements to ERS, FFSS, Voltage Reduction, and Load Shedding provide comparatively smaller reductions in extreme load-shed risk. These findings emphasize that combined investments in Weatherization and network infrastructure yield the highest resilience benefit, while market and operational refinements provide supporting mitigation against severe curtailment events.

D. *Discussion*

The simulation confirms that involuntary load-curtailment risk is seasonal and correlated across multiple system layers. The integrated bow-tie analysis provides a quantitative foundation for resource adequacy and policy evaluation. This implementation includes a BESS degradation trigger but does not yet represent BESS as an explicit mitigative barrier. Future work will model BESS on the mitigative side as energy-limited

979-8-3315-8138-1

reserve injection with availability and state-of-charge constraints, which is expected to compress short-duration scarcity outcomes and alter barrier rankings in high-BESS futures.

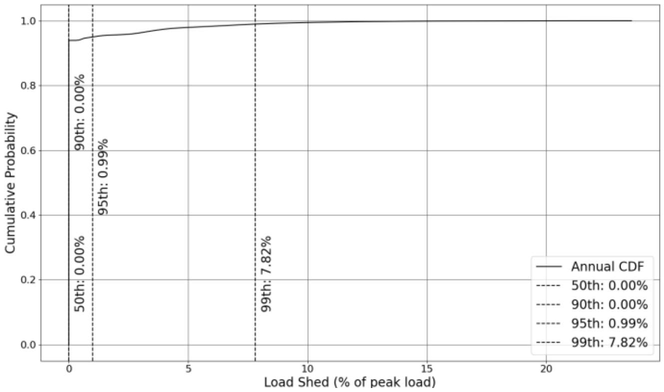

Fig. 3 Cumulative Distribution of Annual Load Shed (%)

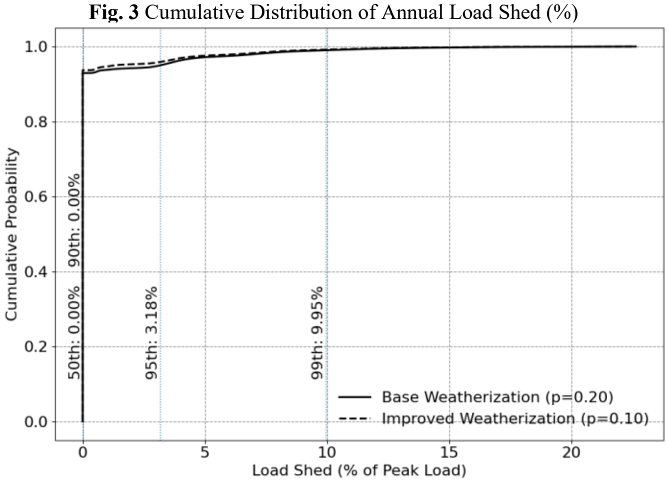

Fig. 4 Monte Carlo CDF of Load-Shed Risk – January Scenario

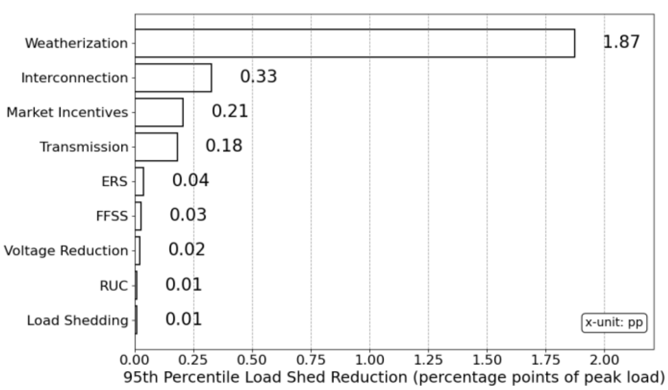

Fig. 5 Barrier Impact on 95th Percentile Load Shed (absolute reduction, percentage points of peak load)

V. Conclusions and Further Work

This paper presents a realistic framework example for analyzing resource-adequacy risk. The results highlight pronounced seasonal vulnerabilities, with the highest risks occurring in January and December, primarily driven by transmission constraints and weatherization vulnerability. The framework does not yet include price-responsive voluntary load curtailment. As a result, the simulated load-shed risk likely represents an upper-bound estimate of involuntary curtailment exposure. Integration of voluntary demand response and behavioral elasticity is planned for future enhancements. Additionally, more comprehensive data analysis is needed to calibrate and refine the probability estimates used in both the root cause and impact analysis components. This includes leveraging historical event data, operational records, and advanced statistical techniques to ensure that the probabilities assigned to triggering events and barrier failures accurately reflect the evolving risk landscape of the electric power industry.

Acknowledgment

The views and opinions expressed in this paper are those of the authors and do not necessarily reflect the official position or policies of the Electric Reliability Council of Texas (ERCOT).

References

[1] U.S. Department of Energy, *Final EO Report on Grid Reliability and Resilience*, Jul. 2025. [Online]. Available: https://www.energy.gov/sites/default/files/2025-07/DOE%20Final%20EO%20Report%20(FINAL%20JULY%207).pdf. [Accessed: Oct. 20, 2025].

[2] Energy Systems Integration Group, "New Resource Adequacy Criteria for the Energy Transition: Modernizing Reliability Requirements" ESIG, Reston, VA, March 2024.

[3] NERC Probabilistic Assessment Working Group (PAWG). Probabilistic Adequacy and Measures Report. North American Electric Reliability Corporation, July 2018.

[4] D. Sun, “Insights into methodologies and operational details of resource-adequacy assessments,” *Energy*, vol. 256, no. 124512, 2022, doi:10.1016/j.energy.2022.124512. ScienceDirect

[5] O. Stover, “Reliability and risk metrics to assess operational adequacy of power systems,” *Electric Power Systems Research*, vol. 223, no. 109452, 2023, doi:10.1016/j.epsr.2023.109452. ScienceDirect

[6] C. Reiz, C. Gouveia, R. J. Bessa, J. P. Lopes, and M. Kezunovic, “Risk Assessment of Future Power Systems: Assuring Resilience of Electrification for Decarbonization,” in *Proc. 12th Bulk Power System Dynamics and Control Symposium (IREP)*, Sorrento, Italy, Jun. 2025, pp. 1–8.

[7] Electric Reliability Council of Texas (ERCOT), Monthly Outlook for Resource Adequacy (MORA) December 2025, Austin, TX, USA, 2025. [Online].https://www.ercot.com/files/docs/2025/10/03/MORA_December2025.pdf. [Accessed: Oct. 20, 2025].

[8] Electric Reliability Council of Texas (ERCOT), *2024 Energy Emergency Alert Overview*, Austin, TX, USA: ERCOT, Aug. 2024. [Online]. Available: https://www.ercot.com/gridinfo/load

[9] A. de Ruijter and F. Guldenmund, “The bowtie method: A review,” Safety Science, vol. 88, pp. 211–218, Oct. 2016, doi: 10.1016/j.ssci.2016.03.001.

[10] J. Zhang, B.-M. Hodge, and A. Florita, “Investigating the correlation between wind and solar power forecast errors in the Western Interconnection,” Proc. ASME 7th Int. Conf. Energy Sustainability & 11th Fuel Cell Science, Engineering, and Technology Conf., Minneapolis, MN, USA, NREL/CP-5500-57816, pp. 1–10, 2013.

[11] ERCOT, “2027 Peak Load Forecast,” ERCOT Grid Info, 2025. [Online]. Available: https://www.ercot.com/gridinfo/load/forecast. [Accessed: Oct. 20, 2025].

979-8-3315-8138-1